Available online at www.sciencedirect.com

SciVerse ScienceDirect

Ceramics International 39 (2013) 5821–5826

CERAMICS INTERNATIONAL

www.elsevier.com/locate/ceramint

Wear resistance of Al_2O_3–CNT ceramic nanocomposites at room and high temperatures

V. Puchy[a,*], P. Hvizdos[a], J. Dusza[a], F. Kovac[a], F. Inam[b], M.J. Reece[b]

[a]*Institute of Materials Research, Slovak Academy of Sciences, Watsonova 47, 04353 Košice, Slovakia*

[b]*Centre for Materials Research, School of Engineering and Materials Science, Queen Mary, University of London, Mile End Road, London E1 4NS, UK*

Received 3 December 2012; received in revised form 13 December 2012; accepted 31 December 2012
Available online 17 January 2013

Abstract

This work describes the microstructure, indentation toughness, room and high temperature tribological properties of alumina–carbon nanotubes nanocomposites with various contents of carbon nanotubes prepared by spark plasma sintering. Materials have been studied by SEM, TEM, Vickers indentation technique on the microhardness and nanohardness testers and, by high temperature ball-on-disk tribometer. The microstructure, CNT dispersion, and fracture surface were studied and wearing mechanisms: fiber pull-out, CNT crushing and formation of transferred film were identified. The addition of 5% CNTs increased the indentation toughness from 3.24 MPa $m^{1/2}$ to 4.14 MPa $m^{1/2}$. The coefficient of friction of alumina–CNT nanocomposites is approximately three times lower in comparison to the alumina monolithic material due to the lubricating effect of carbon nanotubes during sliding.

Keywords: C. Wear resistance; Alumina–CNT nanocomposites

1. Introduction

Nanoscience and nanotechnologies are new approaches of research and development involving precise manipulation and control of atoms and molecules and creating novel structures with unique properties. Advanced ceramics and ceramic based composites/nanocomposites, thanks to their excellent properties, will have a strong position in different fields in new research activities in the field of the ceramic nanocomposites with main attention on the carbon nanotubes/nanofibres reinforced ceramics. Recently a growing need is observed for structural materials with high hardness and wear resistance, high melting temperature, oxidation resistance, chemical stability, etc. The discovery of carbon nanotubes (CNTs) has generated considerable interest owing to their small size, high aspect ratio, low mass and excellent mechanical, electrical and thermal properties. Similar to single-walled and multi-walled CNTs, there are similar carbon based filamentous nanomaterials/carbon nanostructures, e.g., carbon nanofibers with similar properties, but with slightly different sizes. Alumina is the most cost effective and widely used material in the family of engineering ceramics. The raw materials from which this high performance technical grade ceramic is made are readily available and reasonably priced, resulting in good value for the cost in fabricated alumina shapes. With an excellent combination of properties and an attractive price, it is no surprise that fine grained technical grade alumina has a very wide range of applications. Aluminum oxide, commonly referred to as alumina, possesses strong ionic interatomic bonding giving rise to its desirable material characteristics. It can exist in several crystalline phases which all revert to the most stable hexagonal alpha phase at elevated temperatures. This is the phase of particular interest for structural applications. Alpha phase alumina is the strongest and stiffest of the oxide ceramics. Its high hardness, excellent dielectric properties, refractoriness and good thermal properties make it the material of choice for a wide range of applications.

In the last few years new ceramic/carbon nanotube composites have been developed and a number of authors have reported improved mechanical and functional properties in case of ceramic/CNT composites compared to the

*Corresponding author. Tel.: +421 55 792 2447.
E-mail addresses: vpuchy@imr.saske.sk, viiktor.puchy@gmail.com (V. Puchy).

0272-8842/$ - see front matter © 2013 Elsevier Ltd and Techna Group S.r.l. All rights reserved.
http://dx.doi.org/10.1016/j.ceramint.2012.12.100

monolithic material [1–6]. Three main problems have been recognized during these investigations; dispersion of the CNTs in the matrix, densification of the composites and degradation of the CNTs. Conventional mixing of CNTs with the matrix powder requires long milling times which may damage the CNTs. Alternative processing routes have been investigated that result in better dispersions and reduced damage to the CNTs. These include in situ growth of CNTs during the processing or ceramic synthesis in situ on CNTs. Regarding the densification of the composites, authors have mainly used hot pressing (HP) or spark plasma sintering (SPS). Hot pressing often results in incomplete densification because the CNTs inhibit the densification, especially at higher volume fraction of CNTs. It has been reported that using SPS improves densification. The investigations to date have focused mainly on ceramic–ceramic based composites with only limited work on other systems, e.g., ceramic–CNT/CNF/Graphene composites. Therefore the potential advantages of CNT/CNF/Graphene as reinforcing elements are still largely unexplored. Only in the last few years publications have appeared that illustrate the positive effect of carbon nanotubes as reinforcing elements in alumina based composites.

2. Experimental materials and techniques

2.1. Preparation of CNTs and Al_2O_3 powders

The CNTs used in this work were commercially available as multiwall carbon nanotubes (MWNTs), NC-7000, from Nanocyl Inc., Belgium. They were synthesized by the catalytic chemical vapor deposition (CVD) method, and have an entangled cotton-like form. The CNTs had an average outer diameter of 9.5 nm (10 graphitic shells), length up to 1.5 μm and density of 1.66 g cm^{-3}. To monitor the colloidal stability, a 77 mg l^{-1} concentration of CNTs in DMF was hand mixed for 15 s and high power bath ultrasonicated (Engisonic plus, Engis Ltd., UK) for 1 h. It was then hand shaken for another 5 min to remove any gradients produced by non-uniform ultrasonication. The dispersion was then placed in front of a luminescent light box to observe its re-aggregation behavior. The alumina matrix used in this study was commercially available 544833 aluminum oxide nanopowder from Sigma-Aldrich, UK. As supplied by the supplier, the main features of this product are as follows: gamma phase; particle size < 50 nm; surface area 35–43 m^{-2} g^{-1}; melting point 2040 °C; and density 3.97 g cm^{-3}.

2.2. Sintering method of Al_2O_3–CNT composites

The experimental materials were prepared by spark plasma sintering (SPS) at the Queen Mary, University of London, UK by F. Inam and M.J. Reece. The MWNTs were dispersed in DMF via high power bath sonication for 2 h and then hand mixed with alumina nanopowder for another 5 min. The liquid mixture was transferred to another jar filled with zirconia balls (milling media) of two different sizes (10 and 5 mm, mass ratio: 3:2). The jar was sealed and rotation ball milled for 8 h at 200 rpm. The milled slurry mixture was dried at 75 °C for 12 h on a heating plate and then transferred to a vacuum oven (100 °C) for 3 days for complete removal of the dispersant. A solvent trap (filled with ice) was connected between the vacuum pump and the oven. The dried mixture was ground and sieved using a 250 mesh and then returned to the vacuum oven for another 4 days at the same temperature for thorough extraction of the solvent. This lengthy drying procedure was followed because any residual solvent has a detrimental effect on the properties of CNT-reinforced nanocomposites. Dried composite powder was poured into a carbon die and cold pressed at 0.62 MPa for 5 s before sintering. Nanocomposite discs (thickness 2 mm and diameter 20 mm) were prepared by SPS in an HPD 25/1 furnace (FCT Systeme, Germany). A pressure of 100 MPa was applied concurrently with the heating (rate 300 °C min^{-1}) and released at the end of the sintering time, which was 3 min for all the samples. The furnace has a pyrometer focused on a hole close to the sample in the upper punch to measure the processing temperature. The sintering temperature was about 1400 °C. All the samples were slowly cooled to avoid fracture due to thermal shocks and differential contractions.

2.3. Microstructural characterization and mechanical testing

All of the sintered samples were, for microstructural examination, prepared by cutting with the diamond disc, grinding with two grades of silicon carbide papers (nos. 600 and 800) and fine polished using a Planopol/Pedemax automatic polishing machine using diamond grit sizes of 40, 20, 10, 6, 3 and 1 μm diamond compounds. This procedure was used to completely remove the influence of surface grinding and should result in a surface whose properties are determined by the final polishing step. Samples were ground, using SiC paper, down to 4000 grit. Scanning electron microscopy (SEM) was used to observe fractured surfaces in order to determine the grain sizes. The fractured and polished surfaces were coated with a very thin layer of gold and transferred to the SEM (JEOL JSM-7000F, 10 kV, working distance 9–12 mm) for examination. Grain sizes were measured with the aid of the software Image J for Windows. A minimum of 50 readings were taken to measure the grain sizes of each material. Transmission electron microscopy (TEM) was carried on TECNAI G^2 FEG SuperTWIN (200 kV). The electron transparent nanocomposite films (thickness < 100 nm) were prepared by mechanical grinding, polishing, dimpling and focused ion milling. Macro hardness and nanohardness were performed on each sample using hardness tester HPO 250, LECO LM 700AT and nanohardness tester Agilent G200, respectively. Indentation fracture toughness

test was performed on samples with 0, 2 and 5% CNT at a load of 50 N using the Vickers indenter. The calculation of the fracture toughness was made using the Anstis equation:

$$K_{IC} = 0.016 \times \left(\frac{E}{H}\right)^{1/2} \times \left(\frac{P}{c^{3/2}}\right)$$

where E is the modulus of elasticity, H is the hardness and c is the radial crack length generated by Vickers indentation. At least 10 indentation were made for each of the investigated materials.

3. Results and discussion

3.1. Microstructure

The microstructure of the composite is shown at higher magnification in the SEM images of Figs. 1–4. From this it is evident that the microstructure of monolithic ceramic is basically different compared to ceramic–CNT composites due to the ratio of the average ceramic grain diameter. For alumina–CNT composites this ratio is approximately 50 (based on a grain size of approx. 500 nm and a CNT diameter of 10 nm), while for monolithic ceramic it is approximately 200. This means that the matrix grains are located around the CNTs, and no CNTs are located inside the alumina grain. The effect of the CNTs on the functional and mechanical properties will hence be significantly influenced by the interfacial properties of the CNT/matrix grains.

3.2. Mechanical properties

The lower hardness of the composite compared to the monolithic material is mainly dependent on the residual porosity that remains in the material after the sintering, similar to that observed in other investigations [1–3]. Together with the porosity, the clusters of the CNTs are characteristic processing defects present in our material and presented in all of the work dealing with similar composites [4–6]. This indicates the still present difficulties in the preparation of carbon nanotubes reinforced ceramic composites but also the

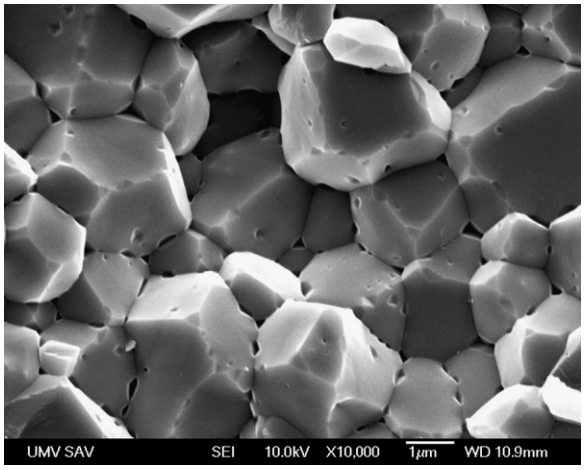

Fig. 1. SEM micrograph of fracture surface of Al_2O_3 monolith.

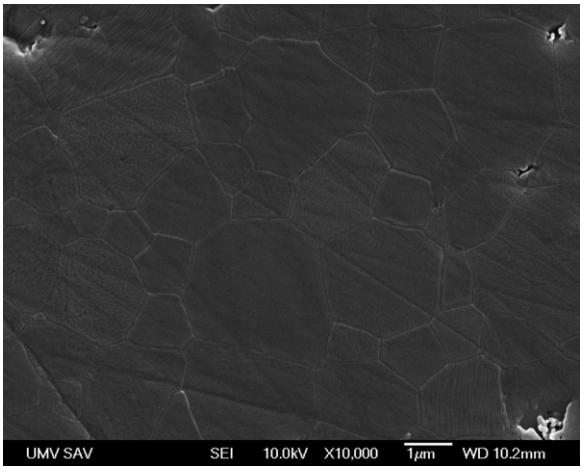

Fig. 2. SEM micrograph of polished surface of Al_2O_3.

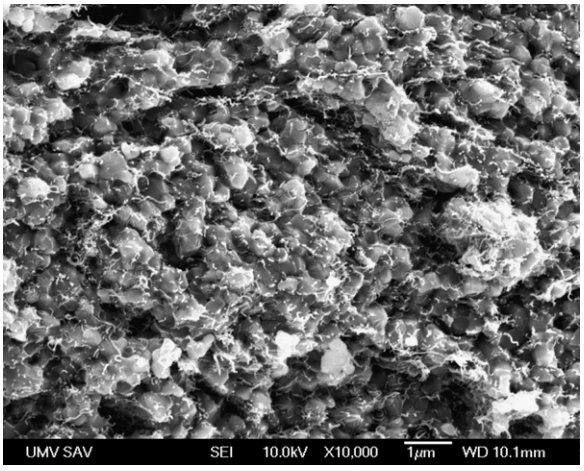

Fig. 3. SEM micrograph of fracture surface of Al_2O_3–5% CNT composite.

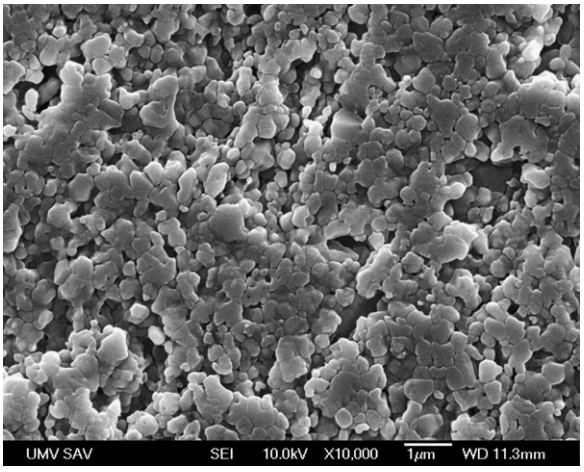

Fig. 4. SEM micrograph of polished surface of Al_2O_3–10% CNT composite.

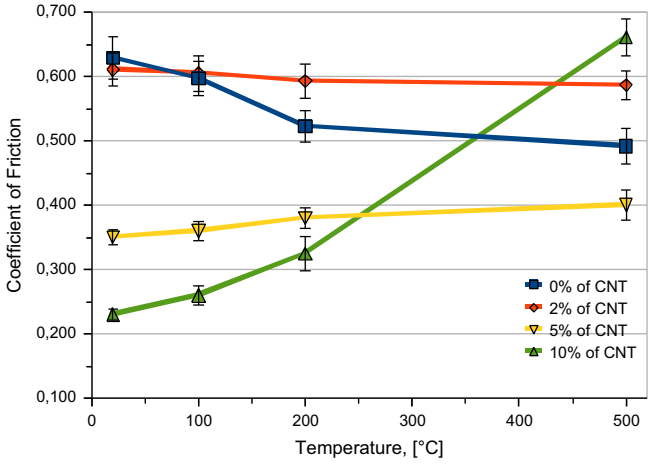

Fig. 5. Effects of temperature on the coefficient of friction for all samples.

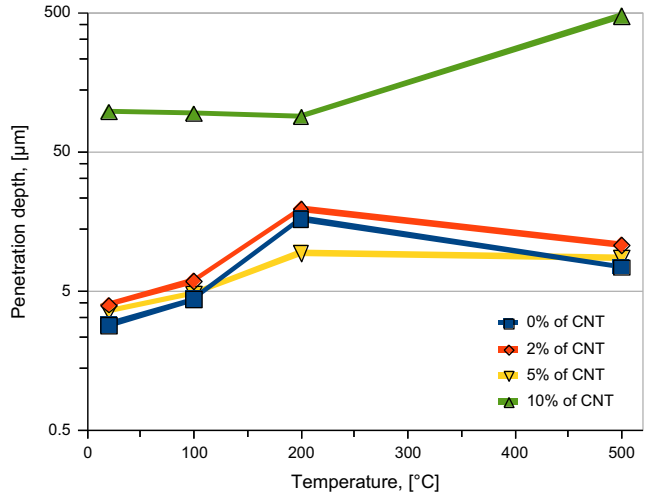

Fig. 6. Effects of temperature on the penetration depth for all samples.

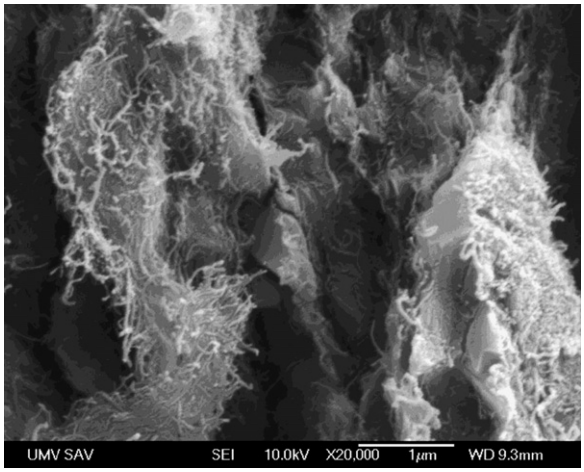

Fig. 7. SEM micrograph of fracture surface of Al_2O_3–10% CNT composite.

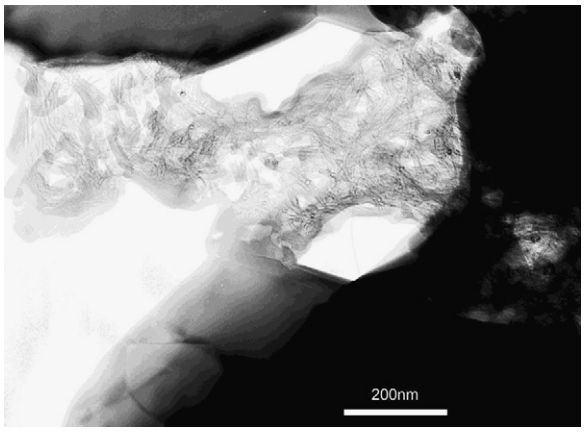

Fig. 8. TEM micrograph of CNTs cluster in Al_2O_3–5% CNT composite.

potential for improvement of their functional and mechanical properties (Figs. 5 and 6).

The SPSed monolithic alumina was fully dense but the alumina–CNT composites were porous, which was associated with clustering of the carbon nanotubes. Relatively large numbers of CNT clusters were observed on the polished, Fig. 4, fracture surfaces of the composites, Fig. 7 and in TEM sample Fig. 8. The size of the clusters varied about a few microns, and porosity was always associated with these clusters. As expected the volume fraction of the clusters was higher in the composites with higher CNF starting content.

3.3. Tribological properties

In the case of alumina composites coefficient of friction by ball on disc technique against alumina ball and penetration depth values at 20, 100, 200 and 500 °C were measured. Instead of investigating wear loss we used depth penetration to find out what is the influence of the CNTs addition into the alumina–ceramic matrix on the tribological properties. Mass loss could not be measured because the samples of alumina wear-tracks were very small and could not be compared with wear-tracks from alumina–CNTs composites. Depth penetration of the alumina samples was about 3 μm therefore the profilometer did not give computed values. The variations of depth penetration and friction coefficient as a function of CNT content and temperature are shown in Table 1. Depth penetration of the alumina composite having 10% CNT increased with an increase in temperature from 30 to 70

Table 1
Microstructural characteristics and main mechanical properties of the nanocomposites.

Material	Grain size Φ 50 (nm)	HV0.05 (GPa)	HV5 (GPa)	K_{IC} (MPa m$^{1/2}$)
Al_2O_3	1900	24.8 ± 3.8	15.71 ± 0.64	3.24 ± 0.15
2CNT	750	8.9 ± 0.6	13.16 ± 0.69	3.84 ± 0.51
5CNT	640	8.5 ± 0.3	7.05 ± 1.37	4.14 ± 0.62
10CNT	310	4.2 ± 0.1	0.72 ± 0.15	n/a

times more as compared to that of alumina monolith specimen having 0% CNT. This enhancement of tribological property also related to the grain size effect and the reinforcement effect of CNTs. Depth penetrations were significantly increased as the CNT content is 10%. This phenomenon could be also explained by the deterioration of the mechanical properties due to dispersing CNTs and poor cohesion. Table 1 suggested that the addition of CNTs has a positive influence on the coefficient of friction but a negative influence on the depth penetration at a 10% CNT content.

Table 1 shows that the friction coefficient of alumina samples decreased gradually as the temperature increased from 20 to 500 °C and also shows that the increased content of CNT in the alumina matrix have a positive effect on the COF. In the case of alumina–CNT composite by lower temperatures the decrease in friction coefficient is due to the lubricating properties of the CNTs (graphite). Furthermore, the rolling motion of CNTs at the interface between the specimen and the ball can probably lower the friction coefficient. In the previous study, this enhancement of tribological properties of the SPSed alumina composites were explained by the grain size effect and reinforcement effect of CNT. On the other hand, it is seen that the increased temperature for alumina–CNTs samples had negative influence on the friction coefficient of composite samples with more than 5% CNT content. The friction coefficient rises sharply at 500 °C mainly in the case of composite with 10% CNT content and is higher than the friction coefficient of alumina samples at room temperature. It is probably caused by the fact that the wear debris consisted of mixture of the CNTs and alumina particles which caused higher friction and dissipation of CNTs by HT. Degradation of depth penetration by CNT addition was also explained by the deterioration of the mechanical properties due to the difficulties in dispersion of CNTs.

Fig. 1 shows the fractured surface morphologies of the alumina–CNT samples. CNTs were agglomerated in grain boundaries of alumina matrix. We can easily expect that this type of agglomeration inhibits reinforcement effect and densification of composite. The shown agglomeration resulted from poor dispersion of CNTs during mixing process and was explained by the difficulty in dispersion and poor cohesion between the CNT and alumina matrix. The pull out of the uniformly dispersed CNTs as well as the superior mechanical properties such as fracture strength of the CNT must contribute to the enhancement of the depth penetration resistance. The coefficient of friction could be influenced by the generated wear debris during sliding. The wear debris is a mixture of alumina and CNT particles. The coefficient of friction shows correlation with depth penetration but further study is needed to understand how the loosened CNT particles influence the frictional behavior.

There is a good correlation between the measured coefficient of friction and the presence of clusters/porosity in the composites processed by SPS. The smaller grain size

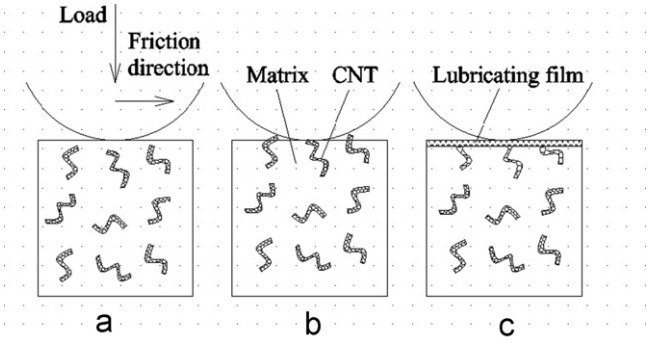

Fig. 9. Schematic diagram of the formation process of self-lubricating film in the alumina–CNT composite.

of the alumina in the composites compared to the monolithic material is evidence that CNTs hinder the grain growth in the composite during sintering. In the SPS process the powder mixture is sintered at moderate pressures and temperatures and in a very short period of time through electric discharge. Such processing conditions preserve the CNTs in the final composites better compared to other techniques. It seems reasonable to suppose that CNTs are more inert than other forms of carbon (CNFs, graphite, and carbon black) and do not participate to any great extent in the sintering of ceramic, which is the reason for the new types of grain boundaries in these composites. A study on finding the solution to densification problems could extend the potentialities of the CNTs in the composites. Characteristic tribological behavior in the alumina/CNT composite is illustrated in Fig. 9.

4. Conclusions

In conclusion, the COF started to decrease only when the CNT content was 5% and more. Microscopic observations of fracture surfaces showed the alumina+CNT composite pulled out CNTs and suggest the making of potentially smeared layer of graphite and crushed CNFs by the friction mechanisms, so called transferred film, which significantly lowers the friction coefficient. The CNTs were effective in creating the transferred film. It may be due to their greater mechanical stability and better distribution throughout the microstructure, Fig. 3. Generally, the presence of CNT tends to decrease the wear resistance due to less than optimal microstructure. However, in the case of Al_2O_3–10% CNT the wear resistance improved, probably dues to significantly reduced friction.

The results showed that the addition of low amount of CNTs into Al_2O_3 not only decreased the friction but also the depth penetration. In Al_2O_3 addition of at least 5% CNT was necessary to decrease the friction but it had beneficial effect to depth penetration which for this system was comparable to that of the monolith. In monolithic materials the dominant wear mechanism was abrasion, in composites with CNT and with higher amount of CNTs (5 and 10%) fiber pull-out occurred with formation of carbon based transferred film over the contact area, which permits

easy shear and helps to create a lubricating effect during sliding.

Acknowledgments

This work was realized within the framework of the project: New Materials and Technologies for Energetics (ITMS: 26220220061), which is supported by the Operational Program Research and Development financed through the European Regional Development Fund.

References

[1] L. Kumari, T. Zhang, G.H. Du, W.Z. Li, Q.W. Wang, A. Datye, K.H. Wu, Synthesis, microstructure and electrical conductivity of carbon nanotube–alumina nanocomposites, Ceramics International 35 (2009) 1775–1781.

[2] E. Zapata-Solvas, R. Poyato, D. Gómez-García, A. Domínguez-Rodríguez, N.P. Padture, High-temperature mechanical behavior of Al_2O_3/graphite composites, Journal of the European Ceramic Society 29 (2009) 3205–3209.

[3] I. Ahmad, A. Kennedy, Y.Q. Zhu, Wear resistant properties of multi-walled carbon nanotubes reinforced Al_2O_3 nanocomposites, Wear 269 (2010) 71–78.

[4] I. Ahmad, M. Unwin, H. Cao, H. Chen, H. Zhao, A. Kennedy, Y.Q. Zhu, Multi-walled carbon nanotubes reinforced Al_2O_3 nano-composites: mechanical properties and interfacial investigations, Composites Science and Technology 70 (2010) 1199–1206.

[5] J.-W. An, D.-H. You, D.-S. Lim, Tribological properties of hot-pressed alumina–CNT composites, Wear 255 (2003) 677–681.

[6] C.N. He, F. Tian, S.J. Liu, A carbon nanotube/alumina network structure for fabricating alumina matrix composites, Journal of Alloys and Compounds 478 (2009) 816–819.